2012-09-06

Analysis of Compensation Techniques Applied to the Control of Converter Connected Synchronous Wind Turbines and DFIG's During Grid Disturbances.

Joseph Kearney
Technological University Dublin, joseph.kearney@tudublin.ie

Michael Conlon
Technological University Dublin, michael.conlon@tudublin.ie

Eugene Coyle
Technological University Dublin, Eugene.Coyle@tudublin.ie

Recommended Citation

Kearney, J.J., Conlon, M.F., Coyle, E. : Analysis of Compensation Techniques Applied to the Control of Converter Connected Synchronous Wind Turbines and DFIG's During Grid Disturbances, 2012, UPEC, London.

Analysis of Compensation Techniques Applied to the Control of Converter Connected Synchronous Wind Turbines and DFIG's During Grid Disturbances.

Joseph Kearney
Dublin Institute of Technology, Ireland
Joseph.kearney@dit.ie

Michael F Conlon
Dublin Institute of Technology, Ireland
Michael.Conlon@dit.ie

Eugene Coyle
Dublin Institute of Technology, Ireland
Eugene.Coyle@dit.ie

***Abstract*- This paper investigates control schemes to improve the performance of converter connected synchronous generators and DFIG's to grid voltage unbalance and grid faults. Both the synchronous generator with a full converter and a DFIG are modelled in Matlab/Simulink. The control schemes of both turbines are modified to improve their performance during grid disturbances including grid voltage unbalance and single-phase faults. These disturbances are introduced into the models at specific times to analyse the performance of the wind generation systems. The performances of both systems to the grid disturbances are compared and the results are analysed.**

***Index Terms*—Synchronous Generator, Converter, DFIG, Voltage Unbalance, Grid Faults, Wind Energy**

I. Introduction

There has been a large increase in the installed wind generation capacity worldwide in recent years, and this has resulted in the necessity that wind turbines remain in operation and connected to the grid in the event of network disturbances. In weak networks, the propensity for grid problems including network voltage unbalance and single-phase faults is higher [2]. The development of WECS in the period from the early 1990's to the present day was predominantly DFIG's, however in recent years the trend appears to be in the direction of synchronous generators. Both types of generators are susceptible to grid voltage unbalance and grid faults [4].

II. SYNCHRONOUS GENERATOR

Synchronous generator excitation field windings can be configured as permanent magnet (PM) or electrically excited, and can be connected to the blades either through a gearbox or directly connected (direct driven).

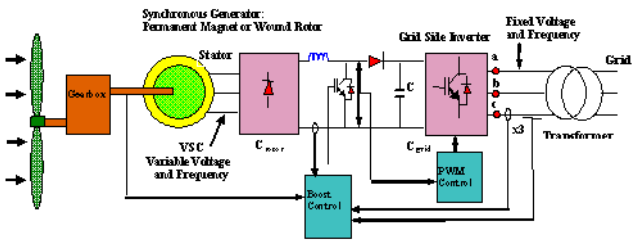

Fig. 1 Synchronous Generator System

The model in this paper is comprised of a wind turbine connected through a gearbox to a synchronous generator, an electrically excited field winding, and a full converter connected to the stator. Rating details are included in Table 1 of the Appendix.

The stator of the synchronous generator is connected to an uncontrolled three-phase rectifier, a DC/DC boost converter, DC link and a three-phase IGBT voltage source inverter, illustrated in Fig. 1.

III. Synchronous Generator Control

The control structure for the grid-side converter is based on the decoupled *dq* vector control method with grid voltage synchronous reference frame. The grid-side converter controls the DC link voltage, converts the DC link voltage to AC and can also control reactive power. The apparent power of the converter can be described as [5, 7]:

$$S \;=\; P_g + jQ_g \;=\; \frac{3}{2} v^{+}_{dqg} i^{+*}_{dqg} \tag{1}$$

where the superscript indicates the positive sequence reference frame.

The real power injected into the grid by the grid side converter in synchronous generator is given as [4, 5]:

$$P_g = v_{dg} i_{dg} + v_{qg} i_{qg} \tag{2}$$

where v_{dq} and i_{dq} are the grid *dq* voltages and currents respectively.

When an asymmetrical fault occurs, positive and negative sequence components can be introduced into (1) as [4, 7]:

$$S \;=\; \frac{3}{2} \cdot \begin{pmatrix} \left(v^{+}_{dqgc+} + v^{-}_{dqgc-} . e^{-j2\omega_e t} \right) . \\ \left(i^{+*}_{dqgc+} + (i^{-}_{dqgc-} . e^{-j2\omega_e t})^{*} \right) \end{pmatrix} \tag{3}$$

Multiplying (3) and expanding yields:

$$\begin{aligned} S = \Big\{ & \left(v^{+}_{dgc+} . i^{+}_{dgc+} - v^{+}_{dgc+} . j i^{+}_{dgc+} + j v^{+}_{qgc+} . i^{+}_{dgc+} + v^{+}_{qgc+} . i^{+}_{qgc+} \right) \\ & + \left(v^{+}_{dgc+} . i^{-}_{dgc-} - v^{+}_{dgc+} . j i^{-}_{dgc-} + j v^{+}_{qgc+} . i^{-}_{dgc-} + v^{+}_{qgc+} . i^{-}_{qgc-} \right) e^{j2\omega_e t} \\ & + \left(v^{-}_{dgc-} . i^{+}_{dgc+} - j v^{-}_{dgc-} . i^{+}_{qgc+} + j v^{-}_{qgc-} . i^{+}_{dgc+} + v^{-}_{qgc-} . i^{+}_{qgc+} \right) e^{-j2\omega_e t} \\ & + \left(v^{-}_{dgc-} . i^{-}_{dgc-} - v^{-}_{dgc-} . j i^{-}_{dgc-} + j v^{-}_{qgc-} . i^{-}_{dgc-} + v^{-}_{qgc-} . i^{-}_{qgc-} \right) \Big\} \end{aligned} \tag{4}$$

Equation (4) can be equated to:

$$P_{acg} = P_{og} + P_{c2g}\cos(2\omega_s t) + P_{s2g}\sin(2\omega_s t)$$

$$Q_{acg} = Q_{og} + Q_{c2g}\cos(2\omega_s t) + Q_{s2g}\sin(2\omega_s t) \qquad (5)$$

where:

$$\begin{bmatrix} P_{og} \\ Q_{og} \\ P_{c2g} \\ P_{s2g} \\ Q_{c2g} \\ Q_{s2g} \end{bmatrix} = \frac{3}{2}\begin{bmatrix} v_{dg+}^{+} & v_{qg+}^{+} & v_{dg-}^{-} & v_{qg-}^{-} \\ v_{qg+}^{+} & -v_{dg+}^{+} & v_{qg-}^{-} & -v_{dg-}^{-} \\ v_{dg-}^{-} & v_{qg-}^{-} & v_{dg+}^{+} & v_{qg+}^{+} \\ v_{qg-}^{-} & -v_{dg-}^{-} & -v_{qg+}^{+} & v_{dg+}^{+} \\ v_{qg-}^{-} & -v_{dg-}^{-} & v_{qg+}^{+} & -v_{dg+}^{+} \\ -v_{dg-}^{-} & -v_{qg-}^{-} & v_{dg+}^{+} & v_{qg+}^{+} \end{bmatrix}\begin{bmatrix} i_{dg+}^{+} \\ i_{qg+}^{+} \\ i_{dg-}^{-} \\ i_{qg-}^{-} \end{bmatrix} \qquad (6)$$

To control the grid-side inverter real power oscillations to zero, it is necessary to put P_{s2g} and P_{c2g} = 0. The reference currents are thus obtained as:

$$i_{dg-}^{-} = \frac{1}{v_{dg+}^{+}}\left[v_{dg-}^{-}.i_{dg+}^{+} + v_{qg-}^{-}.i_{qg+}^{+}\right] \qquad (7)$$

$$i_{qg-}^{-} = \frac{1}{v_{dg+}^{+}}\left[v_{dg-}^{-}.i_{dg+}^{+} - v_{dg-}^{-}.i_{qg+}^{+}\right] \qquad (8)$$

The equations for the synchronous generator demonstrate that during conditions of voltage unbalance, whether as a result of voltage unbalance due to unequal single-phase loads in the locality of the generators or as a result of single-phase faults, the synchronous generator grid converter will be affected. In the grid oriented reference frame, V_{dq} is aligned with the grid voltage and V_{qg} = 0 and (2) is then:

$$P_g = v_{dg} i_{dg} \qquad (9)$$

During asymmetrical network voltage conditions or single-phase faults the power injetced can be decribed as:

$$P_{gF} = v_{dg+}^{+} i_{dg} = v_{dg} i_{dg}\frac{v_{dg+}^{+}}{v_{dg}} = P_g \frac{v_{dg+}^{+}}{v_{dg}} \qquad (10)$$

Where P_{gF} is the power fed to the grid during the disturbance.

Power injected into the grid will reduce according to the ratio of positive sequence voltage to rated grid voltage, however the power supplied by the synchronous generator is unchanged and therefore a power unbalance in the DC link bus results [7].

IV. Control of DC Link Boost Converter

If the synchronous generator speed varies, the DC voltage on the DC link will vary. The boost converter is designed to control the DC link voltage supplied to the inverter. The generator speed and torque are controlled by controlling the pulses to the boost converter, and this in turn controls the DC link inductor current [6, 7]. The power fed from the synchronous generator through the DC link bus to the inverter is thus controlled by the boost converter. The DC link power equation can be described, neglecting losses as:

$$\frac{1}{2} C \frac{dv_{dc}^2}{dt} = P_s - P_g \qquad (11)$$

where P_s is the generator stator real power and P_g is the real power delivered by the grid side converter to the grid.

During the aforementioned grid disturbances (11) will not balance, P_g will decrease whereas P_s will continue to supply generated power form the synchronous generator, and thus the DC link voltage will increase.

The boost converter can be controlled to reduce the DC link current by using:

$$\frac{v_{dg+}^{+}}{v_{dg}} \qquad (12)$$

When a single-phase voltage sag occurs the positive sequence voltage v_{dq+}^{+} will reduce, however the reference voltage v_{dq} will remain as rated, and therefore the reference signal will be reduced as in (12).

The control block diagram of the generator side converter and the grid side converter is illustrated in Fig. 2.

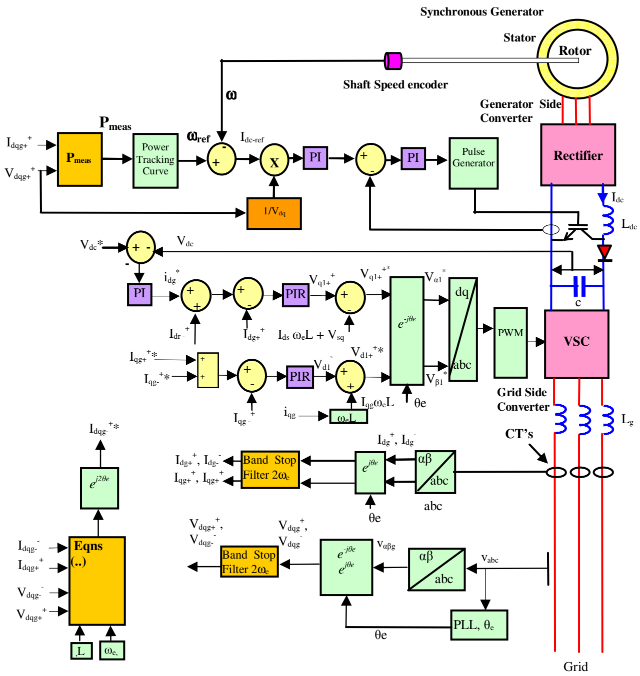

Fig. 2 Synchronous Generator Control

V. Resonant Control of Grid Side Synchronous Generator Converter

The negative sequence control currents I_{dqr}^{-}, (7) and (8) have a frequency of $2\omega_e$ (100 Hz) and to control these currents adequately it is thus necessary to use a controller that is tuned to 100 Hz. A proportional, integral plus resonant (*PI+R*) grid-side converter current controller can be implemented for directly controlling both the positive and negative sequence components of real power [3, 7].

The DC components are regulated normally by the *PI* controller however this controller cannot regulate the double frequency components. The voltage reference output of the *PI&R* controller can be described as [7]:

$$v_{dqg}^{e+*} = \left(i_{dqg}^{e+*} - i_{dqg}^{e+}\right)\left\{k_p + \frac{k_i}{s} + k_{iR}\left(\frac{s}{s^2 + s2\omega_e + (2\omega_e)^2}\right)\right\} \quad (13)$$

In the scheme described by (13) ω_e is the resonant frequency of the controller, and K_P and K_i are the proportional gain and the integral gains respectively. This controller has a very high gain around the resonant frequency and it eliminates the steady state error between the reference and the measured signal.

VI. DFIG

The DFIG generator model considered in this paper is comprised of a wind turbine connected through a gearbox to an induction generator. The rotor of the induction generator is connected to a back-to-back IGBT converter, illustrated in Fig. 3.

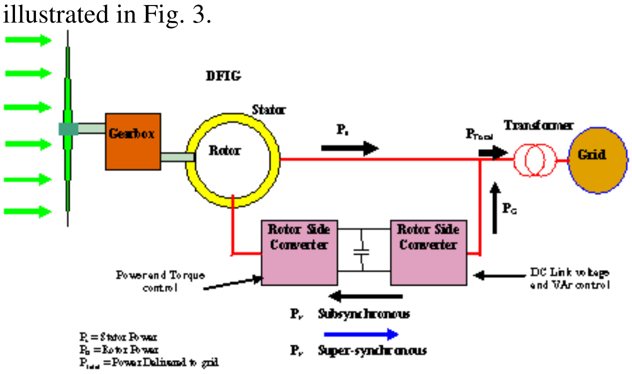

Fig. 3 DFIG

Using the equations for positive and negative sequence voltages and currents the apparent power of the converter can be calculated to improve the effects of voltage unbalance. The stator output apparent power can be described in the positive sequence reference frame as [3]:

$$S = P_S + jQ_S = -\frac{3}{2}V_{dqs}^{+}I_{dqs}^{+*} \quad (14)$$

where the superscript (+) indicates the positive sequence reference frame and $V_{dq}^+ = V_d^+ + jV_q^+$ and $I_{dq}^+ = I_d^+ + jI_q^+$. Equation (14) can be expanded as [3]:

$$S = -\frac{3}{2L_s}\left(\begin{matrix}\left(V_{dqs+}^{+} + V_{dqs-}^{-}.e^{-j2\omega_e t}\right)\left(I_{dqs+}^{+*} + (I_{dqs-}^{-}.e^{-j2\omega_e t})^{*}\right) \\ -L_m\left(V_{dqs+}^{+} + V_{dqs-}^{-}.e^{-j2\omega_e t}\right)\left(I_{dqr+}^{+*} + (I_{dqr-}^{-}.e^{-j2\omega_e t})^{*}\right)\end{matrix}\right) \quad (15)$$

When (15) is multiplied out and expanded in term of d and q positive and negative terms, the terms for active and reactive power can be obtained as:

$$S = P_s + jQ_s = \left(P_{so\_av} + P_{s\sin 2}\sin(2\omega_s t) + P_{s\cos 2}\cos(2\omega_s t)\right)$$
$$+ j\left(Q_{so\_av} + Q_{s\sin 2}\sin(2\omega_s t) + Q_{s\cos 2}\cos(2\omega_s t)\right) \quad (16)$$

where P_{so}, $P_{s\ sin2}$, and $P_{s\ cos2}$, are the DC average, sine and cosine terms respectively, of twice the network frequency contained in the stator active power.

The sine and cosine terms in (16) can be equated to the expansion of (15) and then put equal to zero to obtain reference values for power and torque as illustrated in [3, 8]. The negative sequence I_{dqs} compensating reference values for the power (17), (18) and torque (19), (20) are respectivelly:

$$I_{qr-}^{-} = \frac{2.V_{qs-}^{-}}{\omega_e L_m} + \frac{1}{V_{ds+}^{+}}\left(V_{ds-}^{-}I_{qr+}^{+} - V_{qs-}^{-}I_{dr+}^{+}\right) \quad (17)$$

$$I_{dr-}^{-} = -\frac{2.V_{ds-}^{-}}{\omega_e L_m} + \frac{1}{V_{ds+}^{+}}\left(V_{qs-}^{-}I_{qr+}^{+} - V_{ds-}^{-}I_{dr+}^{+}\right) \quad (18)$$

$$I_{dr-}^{-} = \frac{1}{V_{ds+}^{+}}\left[V_{qs-}^{-}.I_{dr+}^{+} - V_{ds-}^{-}.I_{qr+}^{+}\right] \quad (19)$$

$$I_{qr-}^{-} = \frac{1}{V_{ds+}^{+}}\left[V_{ds-}^{-}.I_{dr+}^{+} + V_{qs-}^{-}.I_{qr+}^{+}\right] \quad (20)$$

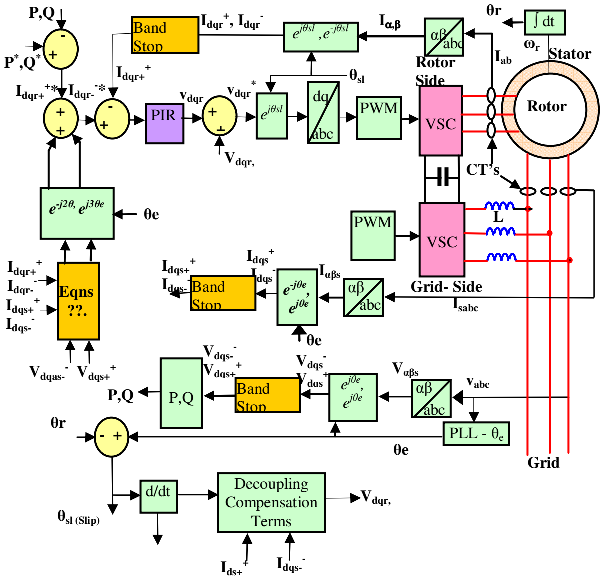

Fig. 4 Rotor Side Converter PIRControl Structure

Similar to the control of the synchronous generator system, resonant controllers can be used to control the DFIG during network disturbances. Fig. 4 illustrates the use of PIR controllers to control the rotor-side converter in a DFIG [3].

VII. SIMULATION STUDY

Both the synchronous generator system and DFIG are in this study modelled in Matlab/Simulink [1]. The system under investigation consists of either generator (DFIG or Synchronous Generator) connected to a simple network as illustrated in Fig. 5.

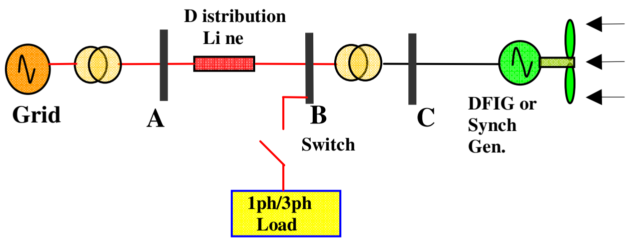

Fig. 5 DFIG/Synchronous Generator Model

Single-phase or three-phase loads can be switched-in for various time periods to simulate various gird faults at bus B in Fig. 5.

VIII. Simulation Results for Power and Torque

In this section responses of the powers of the DFIG and synchronous generator when voltage unbalance is introduced at bus B in Fig. 5 are investigated. In the case of the DFIG voltage unbalance is introduced at 0.5 s and the compensation technique is implemented at 0.6 s. Fig. 6(a) shows the DFIG stator power plot. Stator power oscillations occur when unbalance is introduced at 0.5s, and when the compensation scheme is introduce at 0.6s the oscillations are reduced substantially.

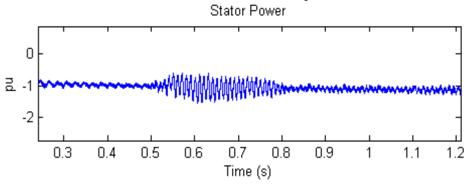

Fig. 6(a) DFG Stator Power

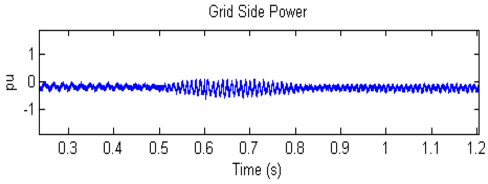

Fig. 6(b) DFIG Grid Side Power

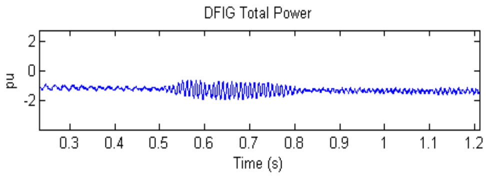

Fig. 6(c) DFIG Total Power Supplied

The grid side converter is controlled to reduce the total power oscillations at the DFIG terminals. There is a good reduction of the grid side converter power oscillations, shown in Fig. (b). The total power delivered by the DFIG to the grid from both the stator and rotor sides is plotted in Fig. 6(c). There is a good reduction in the power oscillations as a result of the grid side converter configured to assist in reducing the overall total power oscillations [3].

The DFIG in the model is connected to the grid at the stator terminals and the grid-side converter; however the synchronous generator system has only one electrical connection to the grid at the converter terminals. In the Simulink model of the synchronous generator system, (Fig. 1), a single phase load is connected at the grid-side of the transformer shown in Fig. 5.

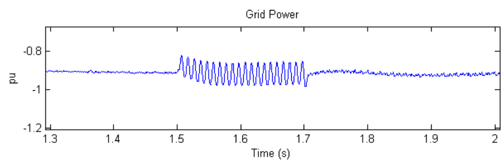

Fig. 7 Synchronous Generator Grid-Side Real Power

Fig. 7 illustrates the grid-side power oscillations measured at the terminals of the grid inverter, occurring at 1.5s when the grid voltage unbalance is introduced at the grid-side converter of the synchronous generator. When voltage unbalance compensation to the grid side converter (Fig.2) is incorporated and switched-in at 1.7s the power oscillations are eliminated.

Fig. 8 is a plot of the DFIG torque with the DFIG input torque set to 0.8 pu. When the voltage compensation is introduced at 0.6 s the oscillations are substantially reduced.

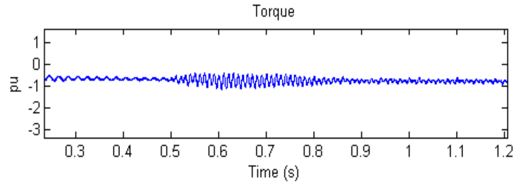

Fig. 8 DFIG Torque

IX. Simulation Results Voltage and Current

The total current supplied by the DFIG is shown in Fig. 9. It is clear that when voltage unbalance is introduced at 0.4s, current unbalance is significant, and when the compensation schemes are switched in at 0.5s the current unbalance decreases and is significantly reduced at 0.8s.

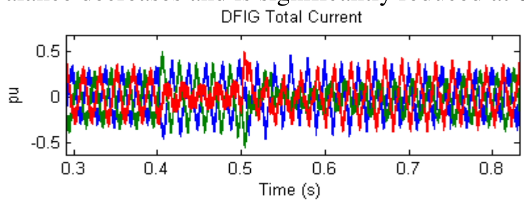

Fig. 9 DFIG Total Current

Similarly the stator current unbalance is also improved as observed in Fig. 10.

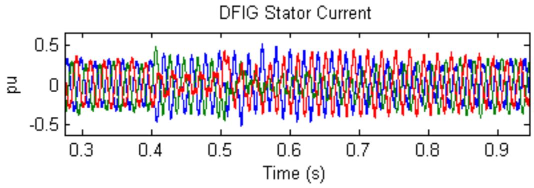

Fig. 10. DFIG Stator Current

Plots of the stator voltage and current at the stator terminals of the synchronous generator are illustrated in Fig. 11.

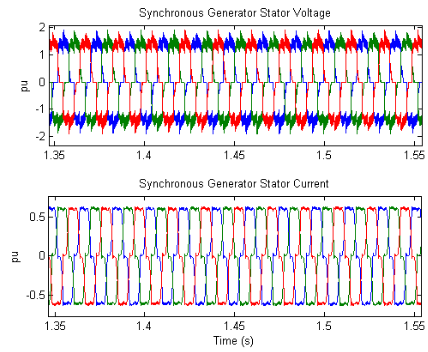

Fig. 11 Synchronous Generator Voltage and Current

It can be observed that during voltage unbalance of 9%, the voltage and current output at the synchronous generator terminals are not affected.

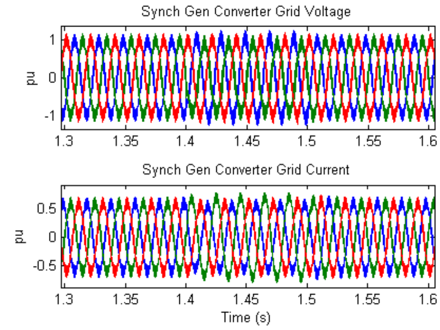

Fig. 12 Synchronous Generator Converter Grid Current and Voltage

The effects of voltage unbalance at the grid side converter of the synchronous generator are illustrated in Fig. 12.

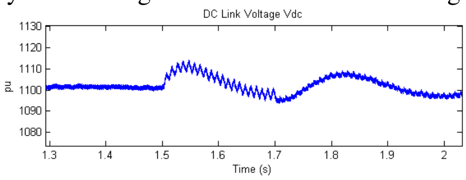

Fig. 13 Synchronous Generator DC Link Voltage

During grid voltage sags close to the synchronous generator system, the power output delivered by the grid side converter is reduced, however the power supplied by the synchronous generator to the converter remains unchanged, which can cause a power unbalance in the converter [**Error! Reference source not found.**]. From (11), it can be observed that when the input power is larger than output power on the DC-side capacitance, the DC voltage will rise, which may have serious impact on normal operation of the whole system and may result in component damage.

Fig. 14 is a plot of the DC link voltage showing the double frequency voltage oscillations occurring at 1.5s when the grid voltage becomes unbalanced. With the introduction of the compensation scheme at 1.7s, the voltage oscillations are eliminated.

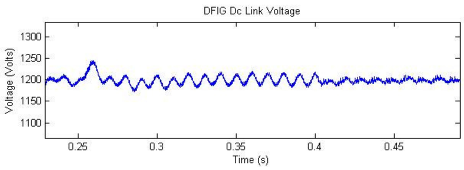

Fig. 14 DFIG DC Link Voltage

Fig. 14 illustrates a similar effect to the DFIG during voltage unbalance introduced at 0.25s and compensation instigated at 0.4s.

X. SIMULATION RESULTS –SINGLE-PHASE FAULT

To mitigate against the effects of single-phase faults at the synchronous generator terminals, the control of the grid-side converter, the boost converter and the blade pitch angle control can be modified. The boost converter can be controlled to reduce the DC link power by reducing the DC link current. To reduce the DC link current, (12) is introduced into the boost control loop, illustrated in Fig. 2. During single-phase faults the positive sequence voltage will drop, and thus the reference signal for the boost converter will be reduced and therefore the current in the DC link will decrease.

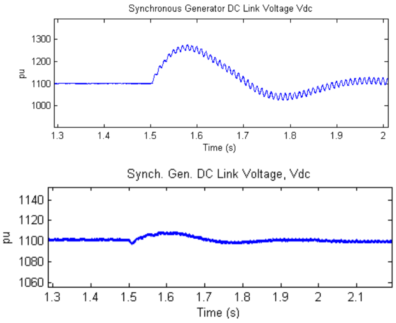

(a)

(b)

Fig. 15 Synchronous Generator DC Link Voltage

Fig. 15(a) illustrates the effect on the DC link voltage V_{dc}, when a single-phase-to-ground fault occurs on the grid-side of the transformer shown in Fig. 1. The DC link voltage rises to approximately 1300V, probably sufficient to damage the converter or trip the protection scheme.

The Simulink model was configured to switch-in both the negative sequence compensation scheme in the grid-side inverter (7) and (8), the PIR control (13), and also the compensation scheme of the DC link boost converter (11) at 1.5s. Fig. 15(b) illustrates the effect of introducing these compensation techniques. The initial amplitude of the rise in the DC link voltage is much reduced and the double frequency voltage oscillations are eliminated.

A similar single-phase fault on the grid side of the transformer at bus B in Fig. 3 for the DFIG was simulated and the result shown in Fig. 16. The negative sequence compensation was implemented at the onset of the fault.

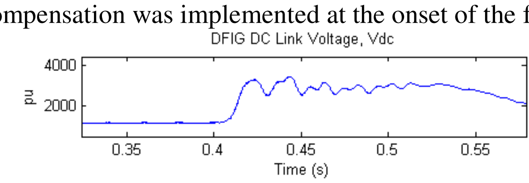

Fig. 16 DFIG DC Link Voltage V_{dc}

The fault was too severe for compensation to be effective. Clearly this level of DC link voltage is unsustainable, and normally the DFIG DC link protection scheme would operate, and trip the DFIG.

The model was also investigated for the effects of a single-phase fault on the synchronous generator power oscillations. A single-phase fault was again introduced into the model at 1.5s. Fig. 17 is plot of the power output at the grid side converter, and large double frequency power oscillations are observed as a result of the fault.

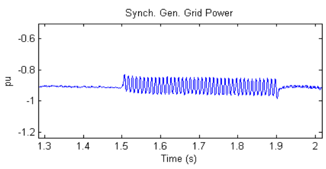

Fig. 17 Synchronous Generator Grid Power Single-phase Fault

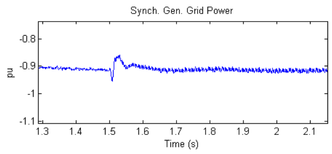

Fig. 18 Grid Power Single-phase Fault

Fig. 18 is a plot of the grid converter power with the compensation scheme (13) switched-in at the onset of the fault. It is clear that the power oscillations as a result of the single-phase fault are eliminated. A similar single-phase was introduced into the DFIG model, however the DFIG compensation technique is not sufficient to control the generator power oscillations as illustrated in Fig. 19.

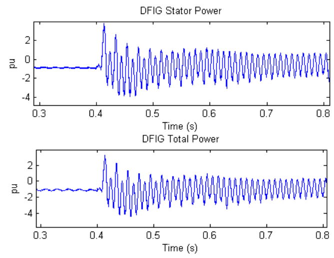

Fig. 19 DFIG Power

XI. Comparison of Performance Response – Voltage Unbalance

Network configurations and parameters in the Simulink models were similar for both DFIG and synchronous generator systems. The performance of both systems to conditions of grid voltage unbalance can be observed in Sections (8) and (9). The real power of the DFIG system is plotted in Fig. 6 and the synchronous generator system grid power is plotted in Fig. 9. The differing responses of both systems to grid voltage unbalance can be explained by their connection configurations. The synchronous generator is not directly connected to the grid. It is connected to a converter, and this in turn is directly connected to the grid. Thus any voltage abnormalities originating in the grid, are not transferred directly to the synchronous generator stator terminals. The DFIG has a direct connection to the stator and a grid side connection to the rotor. It is the direct connection to the stator terminals, and associated low value of negative sequence impedance of the induction generator, that result in large negative sequence current and power oscillations. And therefore the synchronous generator responds better to voltage unbalance when the compensation scheme is introduced.

Fig. 11 shows the generated voltage and current at the stator terminals of the synchronous generator, and it can be observed they are unaffected during voltage unbalance. In contrast the stator of the DFIG is directly connected to the grid, and significant current distortion occurs, illustrated in Fig. 10.

With respect to single phase faults, the synchronous generator system using compensation techniques described, is capable of controlling the large power oscillations whereas the DFIG has limitations and cannot.

XII. Conclusion

A comparison of the performance of a DFIG and a synchronous generator WECS, to the effects of single-phase faults and network voltage unbalance conditions has been investigated. The DFIG is particularly susceptible to single-phase faults and network voltage unbalance, due to the direct connection of the stator to the grid. The negative sequence impedance of the generator is much lower than the positive sequence impedance and with relatively low values of grid voltage unbalance at the DFIG terminals, high unbalanced currents can occur.

The synchronous generator connected to the grid through a converter, is also affected by single-phase faults and grid voltage unbalance, however the synchronous generator system is more robust when compared to the DFIG.

XIII. Appendix

Table 1 Synchronous Generator Parameters

Rated Power	2.0MW	Xd	1.305pu
Frequency	50 Hz	Xd'	0.296pu
Rated Voltage	730V	Xd''	0.252pu
R_s	0.006 pu	Xq	0.474pu
Inertia Constant	5.04s	Xq'	0.243pu
		Xq''	0.18pu

Table 2 DFIG Parameters

Rated Power	1.5MW	R_r	0.005 pu
Frequency	50 Hz	L_{lr}	0.156 pu
Rated Voltage	575V	L_m	2.9 pu
R_s	0.00706 pu	Inertia Constant	5.04s
L_{ls}	0.171 pu	Stator/Rotor turns ratio	0.38

References

1. Matlab. The Mathworks Inc.
2. J Kearney, M. F. Conlon, "Control Double-Fed Induction Generator Wind Turbine During Network Voltage Unbalance Conditions", *42nd Universities Power Engineering Conference (UPEC)*, Padua, Italy, 2nd - 5th September 2008.
3. Joe Kearney, M F Conlon & E Coyle, "The Control of Rotor Side and Grid Side Converters in a DFIG During Network Voltage Unbalance Conditions Using Resonant Current Controllers", EVRE Conference, Monaco, 24th- 28th March 2010, EVER10-288.
4. Xiao-ping Yang, Xian-feng, Yan-li Bai, "Asymmetrical Voltage Dip Ride-through Enhancement of Directly Driven Wind Turbine with Peramanent Magnet Synchronous Generator", Ch Jour 2009.
5. Yang Xiao-ping, Duan Xian-feng, Feng Fan, Tian Lu-lin, "Low Voltage Ride-through of Directly Driven Wind Turbine with Permanant Magnet Synchronous Generator", *IEEE 2009* ..
6. Jin Yang Yajing Gao and John O'Reilly, "Permanent Magnet Synchronous Generator Converter Protection Analysis during DC Wind Farm Open-Circuit Fault Condition", *IEEE* Electrical Power & Energy Conference 2009.
7. J Kearney, M. F. Conlon and E Coyle, "Analysis of Converter Connecetd Synchronous Wind turbines to Grid Disturbances.", 45th Unisversities Power Engineering Conference (UPEC), Soust, Germany, 5th-8th September 2011.
8. Van-Tung Phan, Hong-Hee Lee, and Tae-Won Chun, "An Effective Rotor Current Controller for Unbalanced Stand-Alone DFIG Systems in the Rotor Reference Frame", *Journal of Power Electronics,* Vol. 10 No. 6, November 2010.